

## LONG TERM ANALYSIS OF NON-PHARMACEUTICAL INTERVENTIONS IN SIR MODEL\*

ZUZANA CHLADNÁ<sup>†</sup>, JANA KOPFOVÁ<sup>‡</sup>, AND DMITRY RACHINSKII<sup>§</sup>

**Abstract.** We propose a new epidemiological model, based on the classical SIR model, taking additionally into account a switching prevention strategy. The model has two distinct thresholds that determine the beginning and the end of an intervention and two different transmission rates.

**Key words.** SIR model dynamics, disease prevention, public intervention, switching transmission rate, endemic equilibrium

**AMS subject classifications.** 34D23, 92D30, 92D25

**1. Introduction.** We study a new epidemiological model, based on the classical SIR model, taking into account switching prevention strategies (closing schools, businesses, home quarantine), which are implemented only when the number of infected individuals reaches a critical level and the prevention strategy stops after the number of infected individuals drops under a different threshold. Such a system is called a switching system. Switching systems have been used in many models ranging from mechanics, biology or electrical engineering, [9]. Stability and bifurcation of such piecewise smooth dynamical systems is an interesting research direction, the interaction between a trajectory and borders for discrete events can bring many complex phenomena. The mathematical properties of this model were analyzed in detail in [2]. We proved that each solution converges either to the endemic equilibrium or to a periodic trajectory. Here we present numerical simulations for many possible scenarios (based on the particular combination of the parameters of the model) and indicate some applications to the current COVID-19 epidemic.

We adopt a Susceptible-Infected-Recovered (SIR) model with demographic effects [1], where the population is divided into three different parts: susceptible ( $S$ ), who are healthy but can contract the disease; infected ( $I$ ), and recovered ( $R$ ), who are immune to the disease. Dynamics of the population can be described by the following system of nonlinear differential equations:

$$\frac{dS(t)}{dt} = \mu N - \frac{\beta S(t)I(t)}{N} - \mu S(t), \quad (1.1)$$

$$\frac{dI(t)}{dt} = \frac{\beta S(t)I(t)}{N} - \gamma I(t) - \mu I(t), \quad (1.2)$$

$$\frac{dR(t)}{dt} = \gamma I(t) - \mu R(t), \quad (1.3)$$

---

\* The work of Jana Kopfová was supported by the institutional support for the development of research organizations IČ 47813059.

<sup>†</sup> Department of Applied Mathematics and Statistics, FMFI, Comenius University, Bratislava, Slovakia (chladna@fmph.uniba.sk).

<sup>‡</sup>Mathematical Institute of the Silesian University, Na Rybníčku 1, 746 01 Opava, Czech Republic, (Jana.Kopfova@math.slu.cz).

<sup>§</sup>University of Texas at Dallas, 800 W. Campbell, Richardson, Texas, 75080, United States, (Dmitry.Rachinskiy@utdallas.edu).

where the parameter  $\mu$  denotes the birth/mortality rate,  $\beta$  the transmission rate,  $\gamma$  the recovery rate and  $N$  the population size. The equality of the birth and mortality rates ensures the population size to be constant, i.e.  $S(t) + I(t) + R(t) = N$  for all  $t$ . This assumption allows us to reduce the system (1.1) to the first two equations, with  $R(t) = N - S(t) - I(t)$ .

Transmission rate  $\beta$  is one of the key model parameters. It can be expressed as the product of the number of daily contacts which a susceptible individual has with infected individuals and the probability of transmission during each contact. Parameter  $\beta$  is not directly observable. Many models are based on the so-called *mass action* assumption for transmission, e.g. parameter  $\beta$  is assumed to stay constant during the whole time period in question, e.g. [11]. During the last decades various models have been proposed to make this assumption more realistic. Among them the so-called *saturation effect* was proposed to be included into the model. The incidence rate, namely the term  $\beta SI$  is either modeled as  $\frac{\beta SI}{1+aI}$  or  $\frac{\beta SI}{1+aS}$ , where  $a$  stands for the saturation rate. Some authors even combine these two effects and model the incidence rate as  $\frac{\beta SI}{1+aS+bI}$ , see [5] and [3].

Recently several studies attempting to analyze an effect of the quarantine policies were published. In [4] the authors analyzed the effect of contact reductions using standard well mixed SEIR model. Another implementation of quarantine policy was proposed in [12]. Here authors presented a new extension of SIR model under the assumption that all infected individuals are isolated after the incubation period in such a way that they cannot infect other people. In [8] a stochastic age-structured transmission model has been applied to explore a range of intervention scenarios.

The objective of the two-threshold policy suggested by our model is to navigate the system to the endemic equilibrium and simultaneously keep the number of infected individuals in check, not committing to continuous intervention. The policy is simple enough to make it implementable. Under this policy, it is desirable to minimize the number of switching events that should happen over the time interval from the epidemics outbreak until the system settles at the equilibrium. From this perspective, a trajectory along which the intervention switches on and then off only once seems optimal.

The paper is organized as follows. In the next section we study the equilibria of the model with constant  $\beta$  and its stability. Section 3 is devoted to a preliminary study of a simple situation with only one switch. Section 4 introduces the model with the relay switch and in Section 5 we present numerical simulations for different combinations of parameters. The last section presents the numerical results adapted for the COVID-19. The numerical solutions of nonlinear differential system were obtained with the functions from Python's `scipy.integrate` package.

**2. Stability analysis and equilibria.** As simple calculation shows, the system (1.1) can exhibit two different equilibria: the infection free equilibrium

$$I_* = 0, S_* = N, \quad (2.1)$$

and if  $\beta > \gamma + \mu$  or equivalently  $R_0 := \frac{\beta}{\gamma + \mu} > 1$  also the endemic equilibrium

$$I_{**} = \mu N \left( \frac{1}{\mu + \gamma} - \frac{1}{\beta} \right), S_{**} = \frac{(\gamma + \mu)N}{\beta} \quad (2.2)$$

exists. If  $\beta < \gamma + \mu$ , only the infection free equilibrium is presented, which can be shown to be globally asymptotically stable. If  $\beta > \gamma + \mu$ , the endemic equilibrium becomes globally asymptotically stable. For more details see e.g. [11].

It is also possible to examine the exact type of the equilibrium points from the Jacobian matrix, which in our case is

$$J(S, I) = \begin{bmatrix} -\mu - \frac{\beta I}{N} & -\frac{\beta S}{N} \\ \frac{\beta I}{N} & \frac{\beta S}{N} - (\mu + \gamma) \end{bmatrix}.$$

For the infection free equilibrium

$$I_* = 0, S_* = N \quad (2.3)$$

we have

$$J(S_*, I_*) = \begin{bmatrix} -\mu & -\beta \\ 0 & \beta - (\mu + \gamma) \end{bmatrix}.$$

The eigenvalues are  $-\mu$  and  $\beta - (\mu + \gamma) = (\mu + \gamma)R_0$ , so this equilibrium is a stable node (both eigenvalues are negative) when  $R_0 < 1$  and it is a saddle when  $R_0 > 1$ .

For the endemic equilibrium one can show that

$$J(S_{**}, I_{**}) = \begin{bmatrix} -\mu R_0 & -\frac{\beta}{R_0} \\ \mu(R_0 - 1) & 0 \end{bmatrix}.$$

The eigenvalues of this matrix are supposed to satisfy the equation

$$\lambda^2 + \mu R_0 \lambda + \frac{\beta \mu (R_0 - 1)}{R_0} = 0, \quad (2.4)$$

they are both imaginary, so the endemic equilibrium is an attracting spiral point if the parameters satisfy

$$R_0^3 - \frac{4\beta R_0}{\mu} + \frac{4\beta}{\mu} \leq 0,$$

or equivalently

$$\mu \beta^2 - 4\beta(\mu + \gamma)^2 + 4(\mu + \gamma)^3 \leq 0, \quad (2.5)$$

otherwise it is a stable node.

**3. Simple change in the transmission rate during epidemic.** First we have implemented a simple non-pharmaceutical intervention. We have studied the dynamics of a basic SIR model, where the transmission rate  $\beta$  changes at time  $t_1$  to a lower value and then back at time  $t_2$  to the same rate. This situation corresponds for example to closing schools or applied quarantine when the number of infected people reaches a given number (time  $t_1$ ) and return to normal life after the number of infected drops below a certain level (time  $t_2$ ). The parameters for our numerical analysis are summarized in Table 3.1.

In the first example we propose the following setup:

$$\beta = \begin{cases} \beta_1 & \text{for } t = [0, t_1) \\ \frac{\beta_1}{10} & \text{for } t = [t_1, t_2) \\ \beta_1 & \text{for } t = [t_2, T] \end{cases}$$

Time horizon	$T$	100 days
Population size	$N$	1000
Birth/death rate	$\mu$	0.01/year
Recovery rate	$\gamma$	0.1
Transmission rate	$\beta_1$	0.2

Table 3.1: Model parameters: Notation and values.

The time points  $t_1$  and  $t_2$  are specified as follows:

$$t_1 = \min\{t : I(t) \geq 120\}$$

and

$$t_2 = \min\{t > t_1 : I(t) \leq 50\}.$$

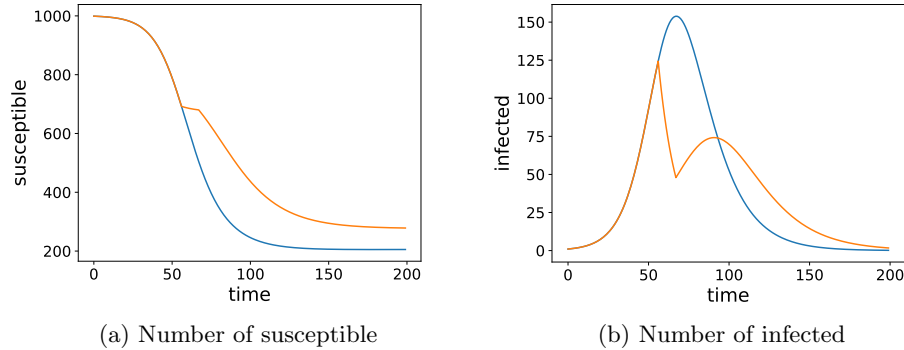


Fig. 3.1: Early stage of epidemics with controlled (blue) and uncontrolled transmission rate (orange).

We observe that even this simple, but carefully chosen, change of the transition rate  $\beta$  during one time interval leads to a significant reduction of the number of infected. One can continue this study and pose an interesting control problem how to determine the switching thresholds so that the number of infected is minimized, but we don't pursue this direction here.

The idea of switching the transmission rate  $\beta$  in a SIR model is not completely new. It was hypothesized that measles epidemics can be controlled more efficiently by a vaccination effort that is pulsed in time rather than uniform and continuous. This policy is called pulse vaccination and it was shown theoretically that if children aged one to seven years are immunized once every five years, this may suffice for preventing the epidemics. The effect of pulse vaccination was studied by many authors, we mention e.g. [1] and [10], where detailed comparison of models with constant and pulse vaccination is provided.

**4. Relay type of change in the transmission rate during epidemic.** A change in the transmission rate  $\beta$  during an epidemic phase might change the final size of epidemic. A change in the transmission rate might be a result of a public health institute intervention or a result of a natural threat of catching the disease.

In our model we assume that a change in the transmission rate is driven by a time evolution of the number of infected individuals. More precisely, we assume, that every time when the number of infected individuals  $I(t)$  exceeds the critical level  $I_1$ , the transmission parameter decreases from its pre-epidemic value  $\beta_1$  to a new value  $\beta_2$ . Once the value of  $I(t)$  declines below the value  $I_2$  the transmission rate returns back to its original value  $\beta_1$ . The question we study here is how the setup of the critical values  $I_1$  and  $I_2$  influences the time development of  $I(t)$  and the final size of epidemic.

The described dependence of the parameter  $\beta$  on  $I$  can be mathematically expressed by the so-called relay hysteresis operator: For the parameters  $I = (I_1, I_2) \in \mathbf{R}^2$  with  $I_1 > I_2$  and  $(\beta_1, \beta_2) \in \mathbf{R}^2$  with  $\beta_1 > \beta_2$ , we introduce the relay operator  $\beta(I, \eta) : C_0([0; T]) \times \{\beta_1, \beta_2\} \rightarrow BV(0; T) \cup C_0^r([0; T])$ ; where  $C_0^r([0; T])$  denotes the space of functions right-continuous on  $[0; T]$ . For any  $I \in C_0([0; T])$  and any  $\eta \in \{\beta_1, \beta_2\}$ ,  $\beta(I, \eta)$  is defined as follows (we write shortly  $\beta(I)$ ):

$$\beta(I)(0) = \begin{cases} \beta_1 & \text{if } I(0) \leq I_1, \\ \eta & \text{if } I_2 < I(0) < I_1, \\ \beta_2 & \text{if } I(0) \geq I_2, \end{cases}$$

for any  $t \in (0; T]$ . Setting  $X_t = \{\tau \in (0, t], I(\tau) = I_1 \text{ or } I_2\}$

$$\beta(I)(t) = \begin{cases} \beta(0) & \text{if } X_t = \emptyset \\ \beta_2 & \text{if } X_t \neq \emptyset \text{ and } I(\max X_t) = I_1 \\ \beta_1 & \text{if } X_t \neq \emptyset \text{ and } I(\max X_t) = I_2 \end{cases}$$

Then  $\beta(I)$  is uniquely defined in  $[0; T]$ , cf. Figure 4.1.

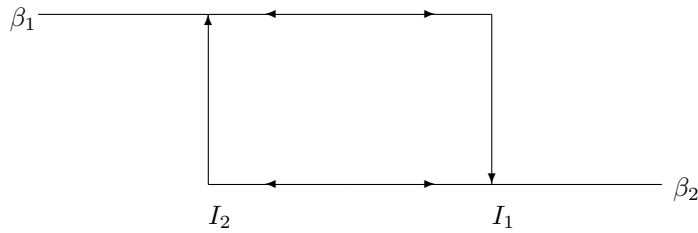


Fig. 4.1: The relay hysteresis operator with thresholds  $I_1$  and  $I_2$ .

The delayed relay operator is a rate independent, piecewise monotone, order preserving and discontinuous hysteresis operator (in any sense). For more details as well as for definitions of different kinds of hysteresis operators, see [7].

According to the proposed type of the non-pharmaceutical intervention we consider SIR model in the following form:

$$\frac{dS(t)}{dt} = \mu N - \frac{\beta(I)(t)S(t)I(t)}{N} - \mu S(t), \quad (4.1)$$

$$\frac{dI(t)}{dt} = \frac{\beta(I)(t)S(t)I(t)}{N} - \gamma I(t) - \mu I(t). \quad (4.2)$$

The global dynamics of this model was studied in [2], but only for the first possibility described in the Numerical experiments Section. We proved that each solution converges either to the endemic equilibrium or to the periodic trajectory. We also showed that to reach a convergence to the endemic equilibrium the lower switching threshold should not be too low. In other words, an intervention decreasing the transmission rate should stop while the number of infected individuals is still not too small. Otherwise, the system can go into a cyclic behavior when the number of infected individuals repeatedly reaches the maximal admissible value. Each time this happens, a new intervention cycle would be initiated.

**5. Numerical experiments.** There are the following possibilities for  $\beta_1 > \beta_2$ :

1. for  $\beta_1$  holds  $R_0 > 1$  and Condition (2.5) is satisfied, for  $\beta_2$  holds  $R_0 < 1$ ,
2. for  $\beta_1$  holds  $R_0 > 1$  and Condition (2.5) is not satisfied, for  $\beta_2$  holds  $R_0 < 1$ ,
3. for  $\beta_1$  and  $\beta_2$  holds  $R_0 > 1$  and Condition (2.5) is satisfied,
4. for  $\beta_1$  and  $\beta_2$  holds  $R_0 > 1$  but Condition (2.5) is not fulfilled,
5. for  $\beta_1$  and  $\beta_2$  holds  $R_0 > 1$  but Condition (2.5) is satisfied only for  $\beta_1$ ,
6. for  $\beta_1$  and  $\beta_2$  holds  $R_0 > 1$  but Condition (2.5) is satisfied only for  $\beta_2$ ,
7. for  $\beta_1$  and  $\beta_2$  holds  $R_0 < 1$ .

In each of the above cases there are further situations depending on the choices of the values  $I_1$  and  $I_2$ .

**5.1. Experiment 1.** First we analyze the first case described in the previous section. For the purposes of the numerical simulation we consider the following values of the parameters:  $N = 1000$ ,  $\mu = 0.01$ ,  $\beta_1 = 0.2$ ,  $\beta_2 = 0.02$ ,  $\gamma = 0.1$ . Further, we set the initial values to be  $I(0) = 1$  and  $S(0) = N - 1$ . Let us note that for  $\beta_1$  the endemic equilibrium ( $I_* = 40.91$  and  $S_* = 550$ ) exists and is a spiral, (condition (5.3) is satisfied), for  $\beta_2$  only the infection free equilibrium exists.

We study the following three cases:

1. Case A:  $I_1 > I_*$  and  $I_2 > I_*$
2. Case AB:  $I_1 > I_*$  and  $I_2 < I_*$
3. Case B:  $I_1 < I_*$  and  $I_2 < I_*$

The results for all three cases are graphically depicted in Figure 3. Figure 5.2 summarizes the corresponding phase-plane diagrams.

**5.2. Experiment 2.** In this numerical experiment we studied the behavior of the system (1.1) in the case that for  $\beta_1$  is  $R_0 > 1$ , but (2.5) is not satisfied, therefore the endemic equilibrium is a stable node. For  $\beta_2$  holds  $R_0 < 1$ .

Here we have proposed the following setup of the parameters:  $N = 1000$ ,  $\mu = 0.01$ ,  $\beta_1 = 1$ ,  $\beta_2 = 0.01$ ,  $\gamma = 0.01$ , initial values are  $I(0) = 1$ ,  $S(0) = N - 1$ . For  $\beta_1$  the equilibrium values are  $I_{**} = 20$  and  $S_{**} = 490$ .

Resulting trajectories in the  $S$ - $I$  plane are depicted in Figure 5.3. Orange curve corresponds to the situation without change in the transmission rate during the whole time period in question. Blue

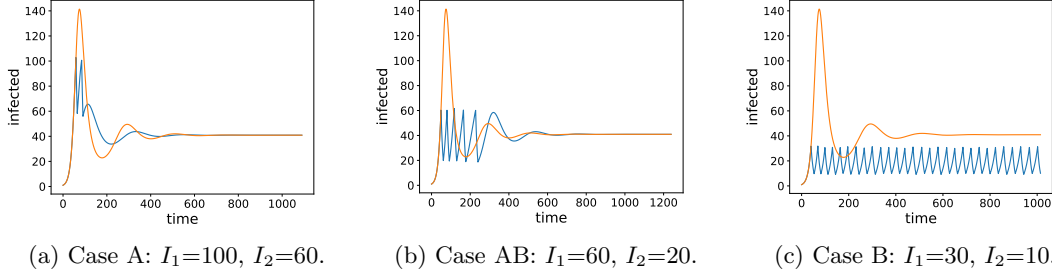


Fig. 5.1: Experiment 1: Number of infected during epidemic with controlled (blue) and uncontrolled (orange) transmission rate

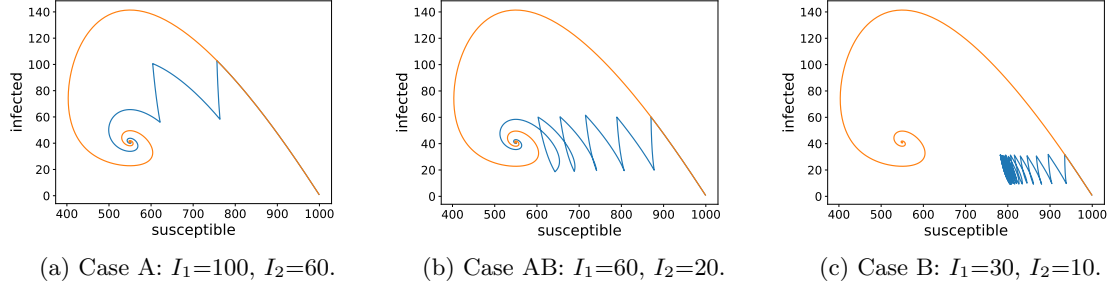


Fig. 5.2: Experiment 1: Phase planes with single trajectories: With (blue) and without (orange) change in the transmission rate.

and green curves represent the situation with the change and two different initial values  $I(0) = 1$ ,  $R(0) = 0$  (blue) and  $I(0) = 5$ ,  $R(0) = 0$  (green).

**5.3. Experiment 3.** In this experiment we have proposed to change the transmission rate in such a way that the existence of the non-zero equilibrium is presented also after the change in the transmission rate, i.e.  $R_0 > 1$  for  $\beta_1$  and  $\beta_2$ . Moreover, we require that the condition (2.5) holds for both  $\beta_1$  and  $\beta_2$ . This can be achieved for instance by the following setup:

$$\beta_1 = 0.2 \text{ with } S^* = 550, I^* = 40.9 \text{ and } \beta_2 = 0.15 \text{ with } S^{**} = 733.33, I^{**} = 24.24.$$

In this setup we have proposed six cases concerning boundary setup for  $I_1$  and  $I_2$  ( $I_1 > I_2$ ):

1. Case AA:  $I_1 > I_*$  and  $I_2 > I_*$
2. Case ABet:  $I_1 > I_*$  and  $I_* > I_2 > I_{**}$
3. Case BetBet:  $I_* > I_1 > I_{**}$  and  $I_* > I_2 > I_{**}$
4. Case BetB:  $I_* > I_1 > I_{**}$  and  $I_2 < I_{**}$
5. Case AB2:  $I_1 > I_*$  and  $I_2 < I_{**}$
6. Case BB:  $I_1 < I_{**}$  and  $I_2 < I_{**}$

Our aim was to analyze the effect of the critical levels setup ( $I_1$ , resp.  $I_2$ ) due to the equilibria

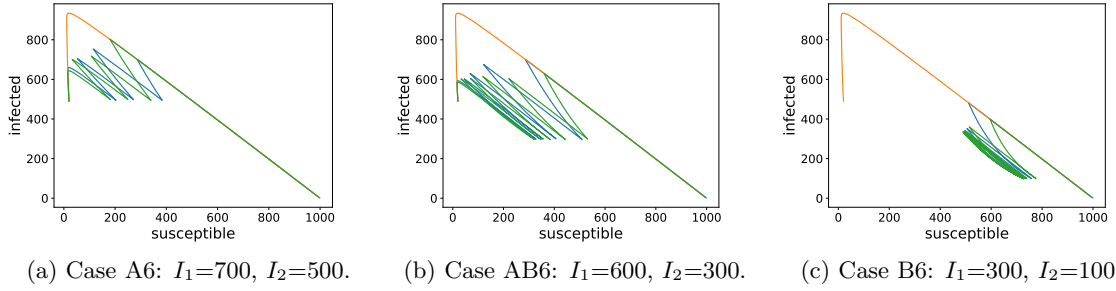


Fig. 5.3: Experiment 2: Phase plane: With (blue, green) and without (orange) change in the transmission rate.

$I^*$  and  $I^{**}$  and compare the behavior of the system with and without  $\beta$  change. Our results are graphically depicted in Figure 5.4.

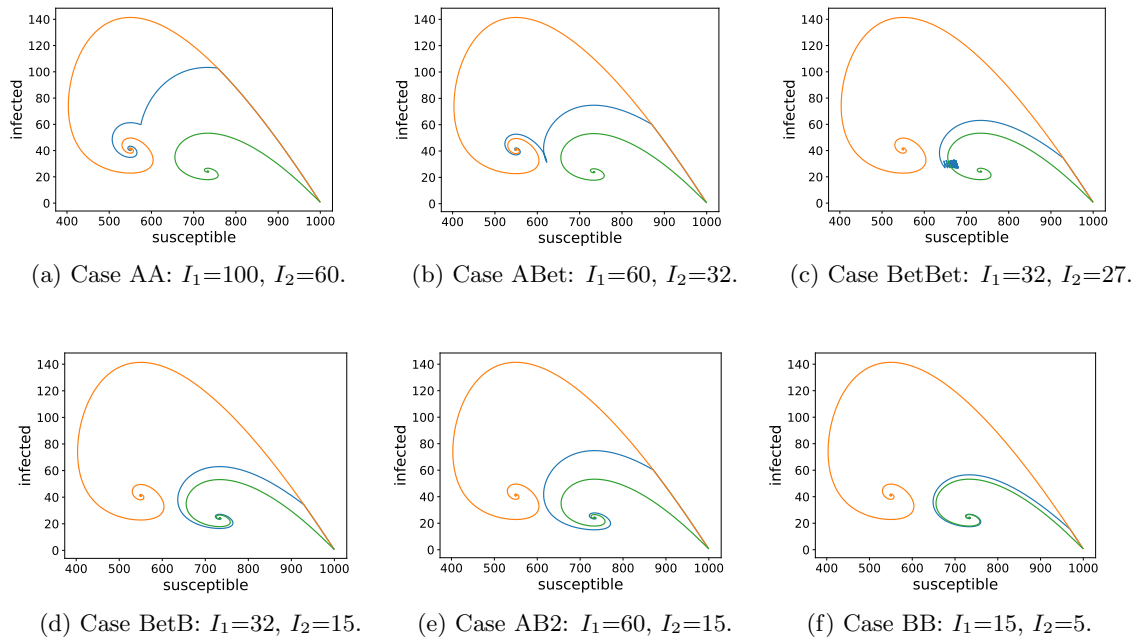


Fig. 5.4: Experiment 3: Phase plane: With (blue) and without (orange) change in the transmission rate. Green curve represents the trajectory of the system with  $\beta_1$ .

**6. Experiment for COVID-19.** Here we perform a case study motivated by the current COVID-19 epidemiological situation in Slovakia. For our purposes we set the modeling population size to be  $N = 5000$ , a small town.

According to [14] birth/death rate in Slovakia ( $\mu$ ) is approxim. 1% per year. Parameter  $\gamma$  is a measure of infectiousness and thus  $1/\gamma$  denotes the length of the infectious period. We assume for COVID-19  $\gamma$  to be  $1/6$ , [8]. Parameter  $\beta$  is not directly observable. The reproduction number for COVID-19 has been estimated to be within an interval (2.5,3). Subsequently, parameter  $\beta$  can be estimated by the relation  $R_0 = \frac{\beta}{\gamma + \mu}$ . In our simulations we use  $\beta = 0.5$ .

It is important to notice here, that for the presented parameters, condition (2.5) is valid due to the fact that parameter  $\mu$  is of lower order than parameter  $\gamma$  (rewriting the condition (2.5) one gets  $\mu R_0 \leq 4(R_0 - 1)(\gamma + \mu)$ ). Moreover, since the reproduction number is greater than one, the endemic equilibrium  $(S_{**}, I_{**}) = (1667, 0.55)$  is an attracting spiral (see Section 2).

In our numerical experiments we assume the realistic initial condition,  $I(0) = 1$ ,  $R(0) = 0$ ,  $S(0) = 4999$ .

Further, we have to set up an epidemic value of the transmission rate ( $\beta_2$ ) as well as the critical levels  $I_1$  and  $I_2$ . The aim of the change in the transmission rate during the epidemic is to eliminate the further disease spread. For the purposes of our study we set  $R_0 = 0.9$ , i.e.  $\beta_2 = 0.15$ . Let us notice here that under the proposed setup of  $\beta_2$  only the disease free equilibrium exists.

Since the value of  $I_{**} < 1$  we have analyzed just the case when both critical levels  $I_1$  and  $I_2$  are above the endemic equilibrium value  $I_{**}$ . In Figure 6.1 we depicted the results of the numerical simulation for  $I_1 = 250$  and  $I_2 = 50$ . As we can observe several waves of epidemics occur (i.e. restrictions rules have to be implemented repeatedly) before the system reaches the endemic equilibrium. Let us note here that lower the threshold value  $I_1$  the longer the time to reach the equilibrium.

In many countries including Slovakia the actual restrictions were performed in a little bit different way, strict quarantine was introduced when the number of infected was very low (or low) and the restrictions were loosen some time after the peak of the epidemic. Other countries, e.g. Sweden or UK introduced regulations later, which corresponds more to our model. However, future policies can be based on our proposed model to keep the epidemic under control. Notice that setting the lower threshold too low is undesirable since it is better to avoid periodic oscillations. Moreover, in the current situation with COVID-19, many countries applied quarantine strategies at different levels and many in 2, 3 or more stages (closing schools, closing businesses, cancelling mass events, etc. ) Also restrictions were cancelled in usually 3 or more stages. This can be modeled by a similar model with 3 (or more) different  $\beta$  parameters and this will be the subject of our future studies.

Finally, due to several special characteristic of COVID-19, for instant a longer incubation period or a presence of a significant number of asymptomatic individuals, the basic SIR model should be extended. Another improvement of corona virus modeling, that we did not include for simplicity in the model, is to consider death rate connected to COVID-19 disease.

#### REFERENCES

- [1] Z. AGUR, L. COJOCARU, G. MAZOR, R.M. ANDERSON, Y. L. DANON, *Pulse mass measles vaccination across age cohorts*, Proc. Natl. Acad. Sci. USA, Vol. 90, (1993), pp. 11698–11702.
- [2] Z. CHLADNÁ , J. KOPFOVÁ , D. RACHINSKII AND S. ROUF *Global dynamics of SIR model with switched transmission rate*, J. Math. Biology, (2020), pp. 1209–1233.
- [3] B. DUBEY, P. DUBEY, US. DUBEY, *Dynamics of an SIR Model with Nonlinear Incidence and Treatment Rate. Applications & Applied Mathematics*, 10(2), (2015), pp. 718–737.

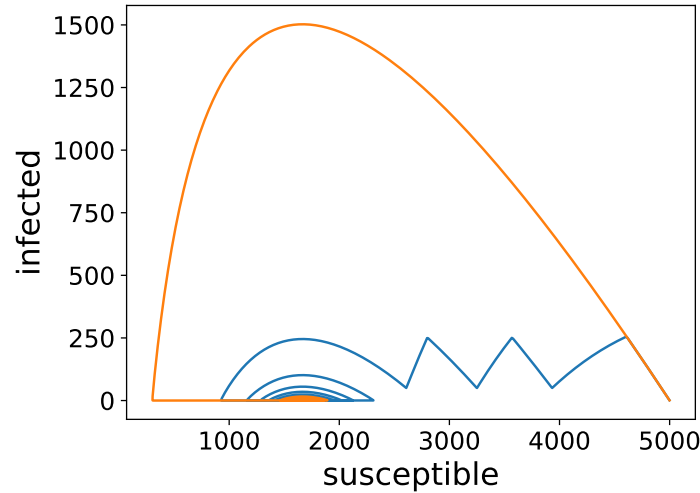


Fig. 6.1: COVID-19 parameters: Phase plane during epidemic with controlled (blue) and uncontrolled (orange) transmission rate

- [4] C. HOU, J. CHEN, Y. ZHOU, L. HUA, J. YUAN, S. HE, Y. GUO, S. ZHANG, Q. JIA, C. ZHAO, AND J. ZHANG, *The effectiveness of the quarantine of Wuhan city against the Corona Virus Disease 2019 (COVID-19): well mixed SEIR model analysis*, Journal of medical virology, (2020), pp. 1–8.
- [5] A. KADDAR, *Stability analysis in a delayed SIR epidemic model with a saturated incidence rate*. *Nonlinear Analysis: Modeling and Control*, 15(3), (2010), pp. 299–306.
- [6] M.J. KEELING, AND PEJMAN ROHANI, *Modeling infectious diseases in humans and animals* Princeton University Press, (2011).
- [7] P. KREJČÍ, *Hysteresis, Convexity and Dissipation in Hyperbolic Equations*, Gakuto International Series Mathematical Sciences and Applications, Vol. 8, Gakkōtoshō, Tokyo, (1997).
- [8] N.G. DAVIES, A.J. KUCHARSKI, R.M. EGGO, A. GIMMA, W.J. EDMUNDS, AND CMMID COVID-19 WORKING GROUP, *The effect of non-pharmaceutical interventions on COVID-19 cases, deaths and demand for hospital services in the UK: a modelling study*, (2020), medRxiv.
- [9] D. LIBERZON, *Switching in Systems and Control*, Springer-Verlag, New York, (1973).
- [10] Z. LU AND X. CHI, *The effect of Constant and Pulse Vaccination on SIR Epidemic Model with Horizontal and Vertical Transmission*, *Mathematical and Computer Modeling* 36 (2002), pp. 1039–1057.
- [11] R. ULLAH, G. ZAMAN AND S. ISLAM, *Stability analysis of a general SIR epidemic model*, *VFAST Transactions on Mathematics*, Vol. 1, N. 1, (2013), pp. 16–20.
- [12] V. VOLPERT, M. BANERJEE, AND S. PETROVSKII, *On a quarantine model of coronavirus infection and data analysis*, *Mathematical Modelling of Natural Phenomena*, 15, (2020), pp. 24.
- [13] A. WANG, Y. XIAO, R.A. CHEKE, *Global dynamics of a piece-wise epidemic model with switching vaccination strategy*, *Discrete Contin. Dyn. Syst. Ser. B* 19, no. 9, (2014), pp.2915–2940.
- [14] *World Bank Open Data*, <https://data.worldbank.org/indicator/SP.DYN.CBRT.IN>